The genomic footprint of climate adaptation in *Chironomus riparius*

Ann-Marie Oppold[1,2], Andreas Wieser[1,2], Tilman Schell[1,2], Simit Patel[2], Hanno Schmidt[2], Thomas Hankeln[3], Barbara Feldmeyer[2], Markus Pfenninger[1,2]

1 Molecular Ecology Group, Institute for Ecology, Evolution & Diversity, Goethe-University, Frankfurt am Main, Hessen, Germany

2 Senckenberg Biodiversity and Climate Research Centre, Frankfurt am Main, Hessen, Germany

3 Institute of Organismic and Molecular Evolution, Molecular Genetics and Genome Analysis, Johannes Gutenberg-University, Mainz, Rheinland-Pfalz, Germany

*Corresponding author: Ann-Marie.Oppold@senckenberg.de

Abstract

The gradual heterogeneity of climatic factors produces continuously varying selection pressures across geographic distances that leave signatures of clinal variation in the genome. Separating signatures of clinal adaptation from signatures of other evolutionary forces, such as neutral processes and adaptation to specific non-clinal conditions of the immediate local environment is a major challenge. Here, we examine climate adaptation in natural populations of the non-biting midge *Chironomus riparius* sampled along a climatic gradient across Europe. Our study integrates experimental data, individual genome resequencing, Pool-Seq data, and population genetic modelling. Common-garden experiments revealed a significant difference in population growth rates corresponding to the population origin along the climate gradient, suggesting thermal adaptation on the phenotypic level. In a population genomic analysis, we derived empirical estimates of demography and migration as parameters for species-specific models to simulate neutral divergence among populations. Despite the effort, the modelling approach consistently underestimated the empirical population differentiation. This highlights important challenges and pitfalls in population genetic modelling of the evolutionary dynamics in multivoltine ectotherms. We instead used a more conservative statistical F_{ST} outlier threshold based on empirical data to infer positive selection across the climate gradient, and combined the results with an environmental association analysis. Through this integration, it was possible to disentangle 999 candidate genes for local adaptation among populations from 162 candidate genes for clinal adaptation along the climate gradients. GO term enrichment analysis revealed that the functional basis of climate adaptation involves the apoptotic process and molecular response to heat.

Keywords: thermal selection, Diptera, population divergence, MSMC, LFMM

Introduction

Among all environmental factors, ambient temperature is most important for ectothermic organisms because it determines the rate of metabolic processes from development to reproduction (Clarke & Fraser 2004). Populations should therefore adapt to local climate and in particular to prevailing local temperatures (Clarke 2003). Moreover, recent evidence suggests temperature to also affect the speed of evolutionary processes driving population divergence (Oppold *et al.* 2016). Compared to specific environmental conditions that are restricted to a respective habitat, as e.g. anthropogenic pollutants, climate factors usually vary gradually across the globe. Thus, the selective pressure resulting from climate variation changes continuously, as can be expected for the evolutionary response of populations along these gradients. Through comparison of multiple populations, patterns of local adaptation should therefore be unique to single populations, whereas adaptation to climate factors should follow clinal patterns.

Evidence for clinal adaptation of phenotypic traits comes from a wide range of taxa, including plants (Loya-Rebollar *et al.* 2013; Silva *et al.* 2014), fish (local adaptation in salmonids reviewed in Fraser *et al.* 2011), invertebrates (response to thermal stress in *Daphnia*, Yampolsky *et al.* 2014), and insects in particular (Fabian *et al.* 2012; Hoffmann & Weeks 2007; Sezgin *et al.* 2004). Intensive research on *Drosophila melanogaster* populations from well-investigated environmental clines gave insight in the large- and fine-scale genomic patterns of clinal variation and its functional contribution to the adaptive phenotype (reviewed in Adrion *et al.* 2015). First applying single markers and later whole-genome data, it was possible to identify candidate genes (e.g. the gene *couch potato* Schmidt *et al.* 2008), and inversions as a form of structural genome rearrangement (Kapun *et al.* 2016) that show clinal variation in allele frequencies. However, little is known about the genomic basis of climate adaptation, particularly in non-model organisms, even though a deeper understanding is expected to bear a central role in the prediction of responses to global climate change (Savolainen *et al.* 2013).

The process of adaptive evolution along clines is not isolated from neutral evolutionary forces or adaptive evolution to local environmental conditions. The confounding influence of demography, introgression and migration present major challenges to investigate the genomic footprint of clinal adaptation (Flatt 2016). Furthermore, non-clinal and endogenous selection needs consideration. For

example, the above mentioned chromosomal inversion pattern in *D. melanogaster* that co-varies with climate was taken as evidence for clinal adaptation (Kapun *et al.* 2016). However, Bergland *et al.* (2016) showed that admixture of different *D. melanogaster* lineages along a latitudinal gradient was primarily responsible for the observed clinal genetic variation (Bergland *et al.* 2014). This introgression might nevertheless be adaptive due to possible pre-adaptation of the respective ancestral lineages to their climatic conditions (Bergland *et al.* 2016). Moreover, endogenous genetic barriers due to disadvantageous genomic combinations that are independent of the environment can coincide with environmental boundaries and mimic the statistical effect of local adaptation (Bierne *et al.* 2011). This highlights the necessity to account for the potential collinearity of demography, adaptation, and endogenous genetic barriers when studying the genomic basis of clinal adaptation.

The non-biting midge *Chironomus riparius* is distributed across most parts of Europe (Pinder 1986). *C. riparius* larvae occur in small streams and ditches, predominantly in agricultural areas, and depending on the local temperature regime, the species produces multiple generations throughout the year (Oppold *et al.* 2016). Common-garden experiments with natural *C. riparius* populations revealed a relative fitness advantage at experimental temperatures matching the respective temperature regime of their origin (Nemec *et al.* 2013). Investigating a climatic gradient from Northern Germany to Southern Spain, this provides a promising system for the analysis of climate adaptation in natural *C. riparius* populations.

Here, we examine temperature adaptation on the phenotypic level and integrate results with population genomic analyses to investigate the genomic basis of climate adaptation in five natural *C. riparius* populations sampled along a climatic gradient across Europe. We conducted common-garden experiments to determine phenotypic differences in several life history traits among populations and confirm their adaptation to different temperatures. Making use of the recently published *C. riparius* draft genome (Oppold *et al.* 2017 in press), we performed genome-scans in a comparative outlier approach to identify signatures of adaptation. Outlier thresholds were obtained from a statistical and a modelling approach based on the demographic population histories inferred by Multiple Sequentially Markovian Coalescence (MSMC, Schiffels & Durbin 2014) and separately estimated migration rates.

A spatially explicit environmental association analysis was employed with the aim of separating the identified signatures of local from clinal adaptation.

Material & Methods

1. Life-Cycle experiments

Phenotypic responses of natural *C. riparius* populations to different temperatures were investigated in life-cycle experiments. Populations were sampled from five locations in the field (Hessen in Germany, Lorraine and Rhône-Alpes in France, Piemont in Italy, Andalusia in Spain, see map integrated in Fig. 1) and established as laboratory cultures (see Oppold *et al.* 2016 for more details). Within the first three generations in the laboratory, we tested for thermal adaptation in full life-cycle experiments at 14, 20, and 26 °C as described in Oppold et al. (2016). We recorded mortality, mean emergence time (EmT_{50}), sex ratio, number of clutches per female, number of eggs per clutch, and fertility of clutches (successful early embryonic development of at least half of the eggs per clutch) to finally calculate the population growth rate (PGR) based on a simplified Euler-Lotka calculation (Vogt *et al.* 2007b). Life-cycle parameters were analysed with two-way ANOVA to test for the effect of temperature, population, and the interaction of both in GraphPad Prism® (v5, GraphPad Software, San Diego, USA). Phenotypic adaptation to different precipitation regimes is far more difficult to test experimentally and we therefore used thermal adaptation as a proxy for phenotypic climate adaptation.

2. Pool-Seq data

We used 100 bp paired-end, Illumina sequencing as Pool-Seq data, derived from 105 to 168 individuals for each population to analyse allele frequency differences and gene flow among populations (see Oppold *et al.* 2017 in press for more details about library preparation, sequencing process, and quality processing of raw data, ENA project number PRJEB19848). Pool-Seq data was mapped to the *C. riparius* draft genome Crip_Laufer (European Nucleotide Archive accession number PRJEB15223, Oppold *et al.* 2017 in press) with BWA using the *bwa mem* algorithm (v0.7.10-r789, Li & Durbin 2009). By increasing the minimum seed length to 30, we managed to obtain highest stringency (as recommended for Pool-Seq, Kofler *et al.* 2011a) while improving mapping success (Supporting information S1, Tab. S1) and drastically speeding up the analysis. The resulting bam-files

were processed according to recommendations for the PoPoolation2 pipeline (v1201, Kofler *et al.* 2011b): sorting (Picard v1.119, available at http://picard.sourceforge.net), removal of duplicates (Picard), removing of low quality alignments (SAMtools utilities v1.1, Li *et al.* 2009), combining all Pool-Seq data sets to one overall *sync*-file, and subsampling the *sync*-file to a minimum coverage of 20X.

3. Inference of demographic population history with individual resequencing data

Demographic population history can be inferred from individual genome data using Multiple Sequential Markovian Coalescence (MSMC2, Schiffels & Durbin 2014). We therefore deep-sequenced the genomes of four randomly chosen female individuals from each population. DNA of adult midges was extracted using the DNeasy Blood & Tissue Kit (QIAGEN, Hilden, Germany). DNA concentration was measured with the Qubit® dsDNA BR Assay Kit in a Qubit® fluorometer and quality was assessed by gel-electrophoresis. Because the total amount of DNA per individual was below 1 µg, preparation of 150 bp paired-end libraries was performed with the KAPA HyperPrep Kit (KR0961, KAPA Biosystems). Libraries were sequenced to an expected mean coverage of 25X on an Illumina HiSeq4000 (BGI sequencing facility, Hongkong). Raw sequences were trimmed and clipped with TRIMMOMATIC (ILLUMINACLIP:adapters.fa:2:30:10:8 CROP:145 LEADING:10 TRAILING:10 SLIDINGWINDOW:4:20 MINLEN:50; v0.32, Bolger *et al.* 2014) and afterwards inspected with FASTQC (v0.11.2; http://www.bioinformatics.babraham.ac.uk/projects/fastqc/). Automated sequential quality checking was performed with a wrapper script to trim the sequences (Supporting information S4: *autotrim.pl*): first round of trimming, inspection of FASTQC results, and repeated rounds of trimming if necessary to remove all overrepresented kmers. Individual resequencing data was mapped with *bwa mem* (*-M -R $individual-read-group*) and processed following the GATK best-practices pipeline (McKenna *et al.* 2010). The detailed pipeline with applied modifications is described in Oppold & Pfenninger (2016).

MSMC2 uses phased haplotype data of single chromosomes as input. We therefore prepared and phased 30 scaffolds with a minimum length of 100 kb for the analyses. Based on the annotation of the draft genome (Oppold *et al.* 2017 in press) in combination with knowledge about the chromosomal location of certain elements or genes, we selected at least one scaffold of each of the four

chromosomes. The scaffolds covered 17.34 % of the draft genome, thus providing a representative genomic overview.

Following the instructions for MSMC2 we used the bamCaller.py (MSMC-tools package) and the respective coverage information for each scaffold of an individual data set (hereafter called 'sample') to generate single-sample VCF-files and mask files. Due to the absence of a *Chironomus* reference panel, all samples (i.e. four samples for each of the five populations) were merged (*bcftools merge*, v1.3, available at https://github.com/samtools/BCFtools) into one VCF containing all two-allelic SNPs for phasing. We used SHAPEIT (v2.r837, Delaneau *et al.* 2013) to phase each scaffold separately accounting for the information of all 20 unrelated samples. SHAPEIT output was reconverted to VCF and samples were separated again (*bcftools view -s sample-ID*).

Mappability masks for each scaffold were generated following the procedure of Heng Li's SNPable program (http://lh3lh3.users.sourceforge.net/snpable.shtml, accessed on 26/01/2017). The phased data per scaffold of two populations and mappability mask of the respective scaffold were combined into one MSMC2 input per scaffold (comprising 2 populations x 4 individuals, i.e. 16 haplotypes). Therefore, ten alternative population-pairs were independently analysed concerning their respective cross coalescence. MSMC2 runs, calculation of effective population size (N_e), and cross-coalescence rates between population pairs followed the general guide of MSMC2 (available on https://github.com/stschiff/msmc/blob/master/guide.md, accessed on 26/01/2017). Since the script to generate the MSMC input (*generate_multihetsep.py*) cannot deal with missing data, there is a slight variation in the combination of sites between different pairs. This also slightly affects the N_e estimation of each population in a respective pair. To overcome this potential bias, the estimations were averaged per time index over the four independent runs per population.

Contrasting to studies with human or *Drosophila* genome sequences, there is no high-quality haplotype data available for *C. riparius*. It is hence not possible to estimate the actual phasing error in terms of the switch error rate (SER). To alternatively decrease uncertainties in the coalescence estimates, we only used time slices with a minimum number of ten coalescence events for downstream analyses. Since *C. riparius* and *Drosophila melanogaster* share similar genetic properties (μ, N_e (Oppold & Pfenninger 2016), chromosome number), we additionally used the conservative SER of

2.1 % from *Drosophila* (Bukowicki *et al.* 2016), corresponding to our sequencing coverage of approximately 20X in a data set with 20 unrelated individuals. To infer the expected mean haplotype length (MHL), genome-wide heterozygosity was estimated as an average of all individuals (number of diallelic SNPs per callable site of the genome). The MHL together with the *Drosophila* autosomal recombination rate of r = 2.1 cM Mb^{-1} (Mackay *et al.* 2012) enabled the calculation of an approximated time horizon (as time to the most recent common ancestor – tMRCA) below which phasing error precludes coalescence rate estimates:

$$tMRCA = \frac{1}{2 \cdot r \cdot MHL}$$

4. Gene flow estimation

To obtain haplotype information for multiple loci from PoolSeq data, we used the individual read information of the data (Pfenninger *et al.* 2015) and extracted 30 loci of 150 bp length, containing at least five SNPs, from the PoPoolation2 F_{ST} output file. For all loci, we considered 15 reads, thus representing haplotypic information of 15 chromosomes. We used Migrate-n (v3.6.5, Beerli 2006; Beerli & Felsenstein 2001) for Bayesian inference of the population mutation parameters (θ) and gene flow rates (number of migrants - N_m) between populations assuming a stepping-stone migration model between the nearest neighbours (MG ↔ NMF, NMF ↔ MF, MF ↔ SI, MF ↔ SS). Parameters were set as described by Pfenninger *et al.* (2015). Based on estimated θ, we calculated the expected N_e for this analysis to convert N_m to an effective migration rate.

5. Simulation of drift expectation

In order to estimate genetic drift under neutral selective conditions and a reasonable population structure, we performed coalescent simulations using fastsimcoal2 (v. 2.5.2, Excoffier & Foll 2011). For each model we sampled 20 sequences of 1 kb length per population, applying a mutation rate per nucleotide and generation $\mu = 4.2 \times 10^{-9}$ (Oppold & Pfenninger 2016), assuming no recombination and a transition bias of 0.595 (Oppold & Pfenninger 2016). The simulations ran for 200,000 iterations per model thus approximating the size of the genome. To account for different length of generation times in different populations (Oppold *et al.* 2016), we corrected N_e according to the respective number of generations per year (G_a):

$$N_e^{adjusted} = \frac{N_e \cdot G_a}{mean\ G_a}$$

Three different demographic models were tested (Supporting information S2). The basic model (*constant*) is based on a branching event of an ancestral population into five subpopulations of constant size 125,000 generations ago. Migration between neighbouring populations was allowed to varying degrees, with high migration rates from Southern France to Northern France and Southern Spain, while in accordance to the gene flow estimation, back migration is occurring more rarely (Supporting information S2).

The *growth* model retained most parameters of the previous model, adding a population growth rate of 1.0×10^{-5}. In this model, every subpopulation accordingly expanded in size since they split 125,000 generations ago.

The final model *approximated* a demographic history with population sizes and migration rates according to the results of the MSMC analysis (see below). Population history was divided in six epochs, with symmetric migration between neighbouring populations.

Finally, we calculated pairwise F_{ST} values between each pair of simulated populations using Arlequin (v3.5, Excoffier & Lischer 2010) and compared the density functions of modelled and empirical F_{ST} values.

6. Population differentiation in 1 kb-windows

Population differentiation was inferred from Pool-Seq data. SNPs from the subsampled *sync*-file were called in a sliding window approach with size of 1 kb to calculate pairwise F_{ST} values (PoPoolation2: *fst-sliding.pl* --min-count 4 --min-coverage 10 --max-coverage 51,38,67,50,45 --pool-size 336:224:210:310:236 --window-size 1000 --step-size 1000 --min-covered-fraction 0.5). We defined the upper 1 % tail of the F_{ST} distribution as statistical threshold for non-neutral differentiation (see below). All 1 kb-windows with F_{ST} above this threshold, as well as above the alternative thresholds from our simulation study (see above), were extracted for downstream analyses.

Separately, Fisher's p-values were calculated for each 1 kb-window (PoPoolation2: *fisher-test.pl* --min-count 4 --min-coverage 10 --max-coverage 51,38,67,50,45 --window-size 1000 --step-size 1000 --min-covered-fraction 0.5). To account for multiple testing, we applied the Benjamini-Hochberg

correction (Benjamini & Hochberg 1995) to all p-values (R-Core 2015). Outlier windows that remained significant after FDR correction ($q < 0.01$) were finally considered as highly divergent.

To investigate the genomic landscape of divergence, adjacent divergent 1 kb-windows were joined to larger divergence regions, as described in Pfenninger et al. (2015). Starting from the first outlier window encountered along a scaffold, adjacent windows were joined to an outlier region in both directions until the mean F_{ST} of the next window dropped below the cut-off value (5 % tail of the F_{ST} distribution). Then the next, not yet joined outlier window was searched and the process repeated.

7. Tajima's D analysis

To analyse the evolutionary forces acting on the identified outlier windows, we estimated Tajima's D (T_D) in 1 kb-windows in each of the five Pool-Seq data sets. We used the PoPoolation tool package (Kofler *et al.* 2011a) with high stringency settings for T_D estimation. We extracted T_D per population for windows that were previously identified as outliers, and investigated these in a population-comparison. T_D values ±1 were conservatively defined as threshold above/below which we expected non-neutral processes, considering following scenarios for a comparison with *n* populations (modified from Pfenninger *et al.* 2015): (i) negative T_D in one to *n*-1 populations is indicative for a selective sweep in the respective population, (ii) negative T_D in all populations is indicative for strong purifying selection, (iii) positive T_D is indicative for balancing selection in the respective population. With Chi^2 tests (*chisq.test* R package) we compared the occurrences of different signatures of selection in population-pairs and afterwards applied the Benjamini-Hochberg correction for multiple testing (*p.adjust* R package).

8. Environmental association analysis

We tested the Pool-Seq data on correlation of environmental variables with genomic differentiation using LFMM (Latent Factor Mixed Model in the frame of the 'LEA' R-package, Frichot & Francois 2015; Frichot *et al.* 2013) to partition clinal from local adaptation. This environmental association analysis (EAA) tool has been shown to provide the best compromise between power and error rates across various scenarios (de Villemereuil *et al.* 2014). To generate the environmental input data, we extracted the complete set of current climate conditions for each sample location from WorldClim

(Hijmans *et al.* 2005). To obtain meaningful, low dimensional environmental parameters, we performed a PCA (principal component analysis, software package PAST v. 3, Hammer *et al.* 2001) on all parameters (WorldClim data including BioClim data, approx. 1950-2000, Hijmans *et al.* 2005). The first three components explained 89 % of total variability and could be related to the following climatic factors (Supporting information S1 Fig. S1-2, Tab. S2): PCA1 – gradient of cold temperatures (58 %); PCA2 – precipitation gradient (21 %); PCA3 – gradient of warm temperatures (10 %).

LFMM allows allele-frequencies from Pool-Seq data as genetic input for the EAA. To avoid spurious correlations, we included only a predefined subset of genomic loci into the analysis by considering all SNPs (SNP call with *snp-diff.pl* from PoPoolation2 with the above settings) that fell in the upper 1 % tail of the population pairwise F_{ST} distribution (estimated as described above with --window-size 1 and --step-size 1) and calculated the allele frequency of the major allele in each population for all SNPs (i.e. this includes all SNPs that exceeded the F_{ST} threshold in at least one population comparison).

LFMM cannot take the pool size of Pool-Seq data into account, which reduces the power of the analysis. Referring to the Bayenv approach (Günther & Coop 2013), we artificially increased our sample size by multiplying each pooled set of frequencies with n_i, where n_i is the sample-size of pool I at this locus (i.e. in our case 20X, see above). The Pool-Seq approach assumes that each read covering a certain position originates from a different haploid chromosome. Therefore, the coverage in our data represents the number of independent chromosomes per population that were used to calculate the respective allele frequency (Futschik & Schlötterer 2010). Correspondingly, we resampled each allele frequency per population for $n_i = 20$ from a simulated beta distribution at each locus: $beta(F_{il} \times n_i + 1, (1 - F_{il}) \times n_i + 1)$, with F_{il} being the empirical frequency at locus l in pool i. This resulted in a genetic data set of 20 simulated individual allele frequencies per population at each locus. To adjust the environmental input to this resampled genetic input without creating artificial environmental variability, we only replicated each environmental factor 20 times for each locus.

We ran LFMM with five repetitions, separately for each environmental factor and a latent factor of K = 5 (i.e. number of populations). Downstream analysis of the LFMM output followed the authors' recommendations for the tool (Frichot & Francois 2015).

9. Functional enrichment analysis

To define putative functional properties of differentiated genomic regions, genomic coordinates of outlier windows from population comparisons as well as clinal candidate loci identified with LFMM were compared with coordinates of protein coding genes in the *C. riparius* draft genome (Oppold *et al.* 2017 in press). We used a custom perl-script to assign windows or loci located within a 500bp up- and downstream region of a gene. To test for gene ontology (GO) terms significantly enriched in genes lying in these regions, we intersected the lists of gene hits to produce different comparisons: gene hits of all population comparisons with gene hits from all environmental correlations (pop-pairs ~ env-variables), gene hits clinal to environmental variables amongst each other (precipitation ~ temp_cold ~ temp_warm), gene hits from outlier windows specific for one particular population for comparison against the other populations. GO terms and KEGG pathways were annotated to all protein sequences using InterProScan (v5.20-59, Jones *et al.* 2014), resulting in a complete set of terms as reference for the functional enrichment analysis. The enrichment analysis was carried out with the topGO R package (Alexa & Rahnenführer 2016) in the category 'biological processes', using the weight01 algorithm and fisher statistics. Enriched GO terms were retained with a p-value of ≤ 0.05.

Results

1. Life-cycle experiments

Full life-cycle common-garden experiments revealed different responses of the populations to the three test temperatures. Corresponding to their position on the European temperature gradient, the two Northern populations (Hessen MG and Lorraine NMF) had higher population growth rate (PGR) at 14 °C than the three remaining populations from warmer locations further South (Rhône-Alpes MF, Piemonte SI, Andalucia SS), whereas this pattern was inverted at 26 °C (Fig. 1).

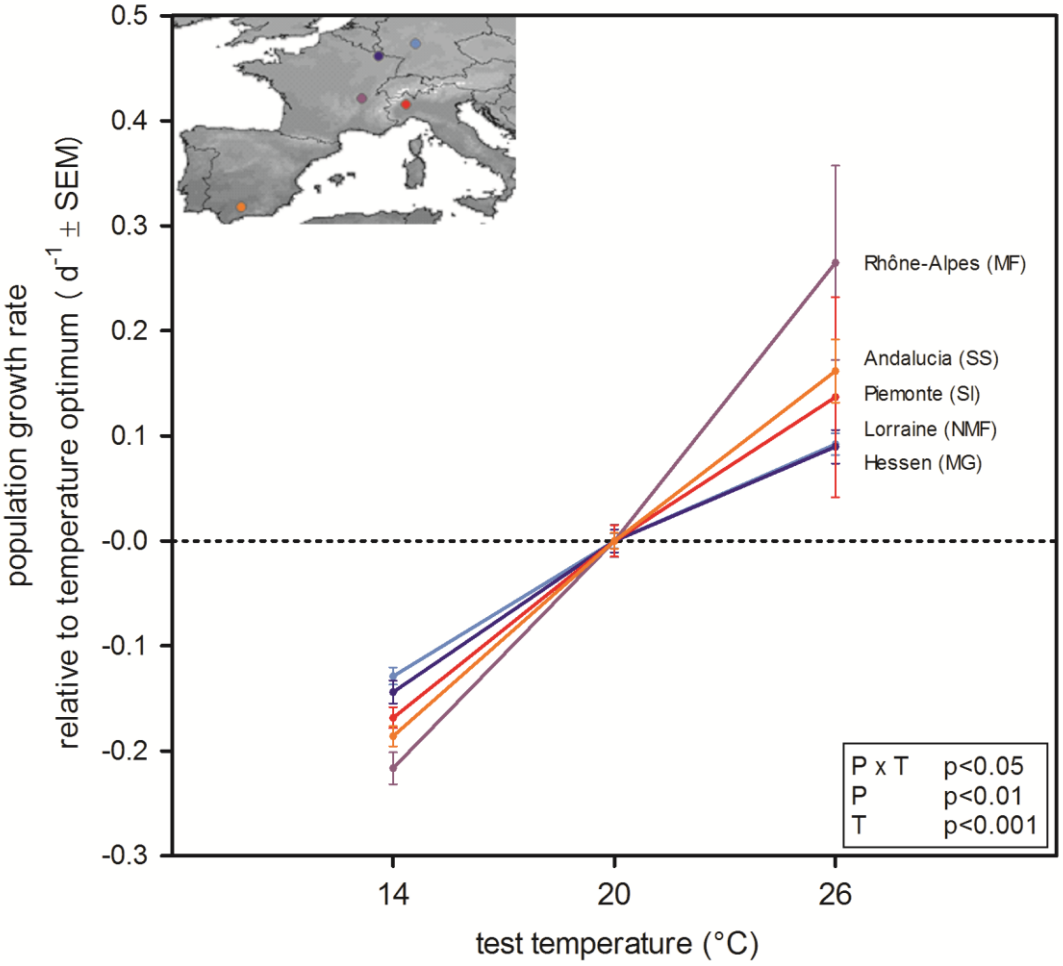

Figure 1: Population growth rate (PGR) of the natural *C. riparius* populations at different test temperatures. 20 °C constitute standard laboratory conditions and were chosen as optimal temperature to normalize the data for the tested populations, since we found overlapping variability (95 % CI) of the PGR in all populations. Locations of the populations along the European climate gradient are shown on the integrated map with the respective colour code. P-value thresholds of two-way ANOVA are given in the box: effect of population (P, $F = 4.782$), temperature (T, $F = 105.4$), and interaction of both factors (P × T, $F = 2.418$).

The differences in PGR between the five populations were based on different underlying life-cycle parameters for warm and cold test temperatures. At 14 °C mortality was significantly lower in the two Northern populations compared to the three remaining populations (Supporting information S1 Fig. S3-A and Tab. S3-A). Furthermore, the two Northern populations showed a tendency of producing more fertile clutches per female at 14 °C than their relatives from more Southern locations (Supporting information S1 Fig. S3-C and Tab. S3-C). These two parameters, however, show increased variability at 26 °C and there was no clinal pattern. The number of eggs per clutch did not differ between temperatures or treatments (data not shown).

As expected for an ectothermic species, temperature had a significant effect on the PGR of the populations and accounted for 68 % of the total variance ($F = 105.37$, $p < 0.0001$). This effect was mainly driven by the temperature-dependent development of the larvae (Supporting information S1 Fig. S3-B, Tab. S3-B). Furthermore, the PGR at the three test temperatures differed significantly between populations explaining 6.2 % ($F = 4.78$, $p < 0.002$) of the total variance, as well as the combined effect of temperature and population (6.3 % of the total variance, $F = 2.42$, $p < 0.025$).

2. Demographic population history and migration

After trimming the coalescence rate estimates from MSMC2 according to our quality threshold of a minimum of ten rate estimates per time slice, the informative time horizon for the inference of the demographic population history stretched from approximately 1,000 to 150,000 generations in the past. Based on a mean heterozygosity of 0.00426 and a switch error rate (SER) of 2.1 %, haplotypes of a mean length of 11,746 bases are informative for this analysis in *C. riparius*. This results in a tMRCA of 2,027 generations, giving a similar threshold of coalescence resolution in the recent past as derived after quality trimming coalescence rates.

In the late past, i.e. approximately 150,000 generations ago, N_e was estimated to an average of about 3.7×10^4 individuals (Fig. 2A). During these generations the relative cross-coalescence between population-pairs revealed a good mixture of all populations with only a slight divergence drop about 100,000 generations ago (Fig. 2B). This ancestral population experienced a threefold decrease in N_e until 10,000 generations ago and by then the populations split during the following 9,000 generations. More or less complete population separation is estimated to have been established 1,000 generations

ago. During time of population separation until 1,000 generations ago, N_e constantly increased reaching an average effective population size of 1.17×10^5. Estimations for younger time points are ambiguous due to the limit of resolution of the analysis.

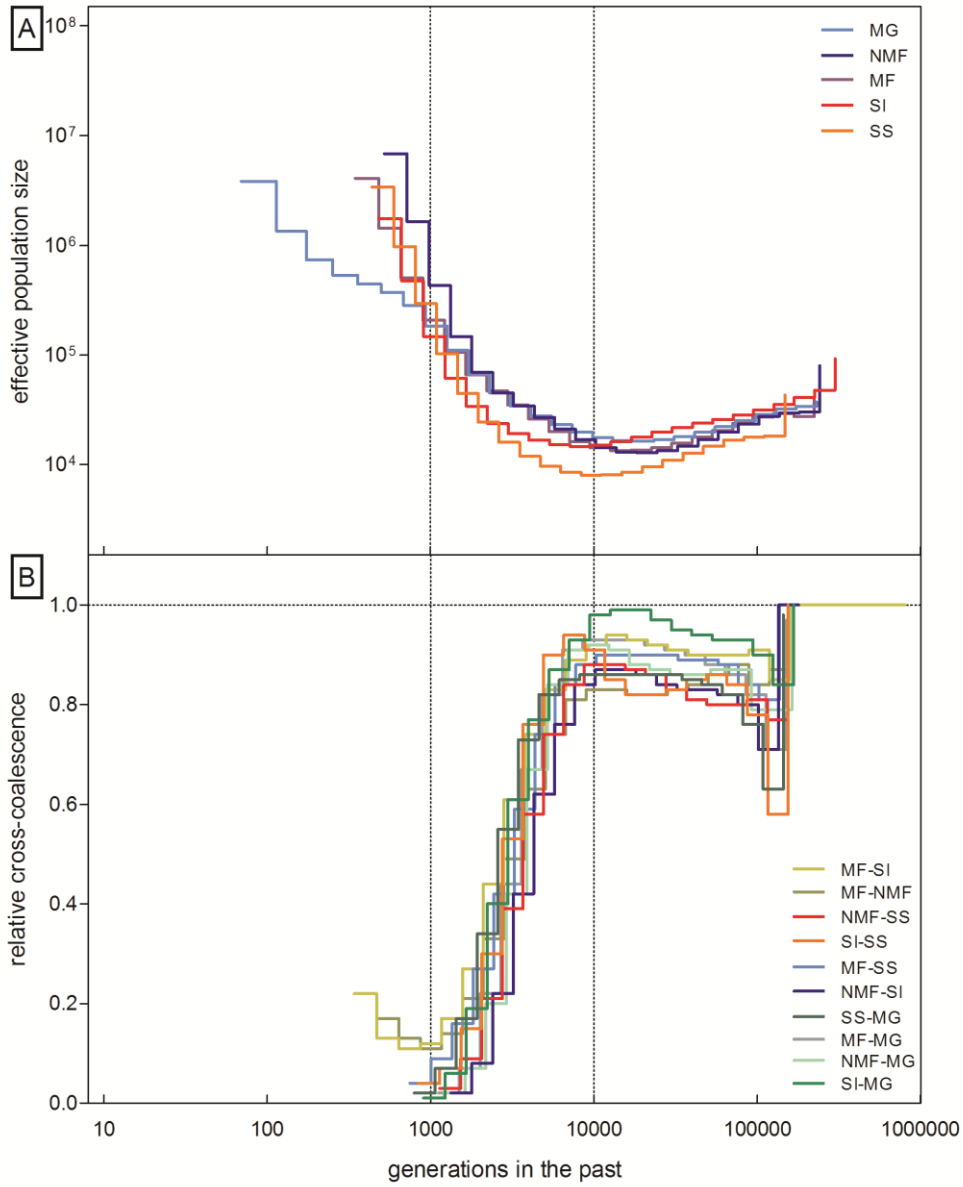

Figure 2: Results from genome-wide MSMC with eight individual haplotypes per population. (A) Effective population size and (B) relative cross-coalescence as indicator for population separation. To account for possible phasing error affecting the resolution, we only retained time indices with a minimum of ten coalescence rates.

The gene flow estimation integrated over the time period available for the analysis, revealed high migration rates, ranging from 3×10^{-5} to 9×10^{-4} (Supporting information S1 Tab. S4). Migration tended to radiate from the geographically centred population MF (Lyon), with less back migration. Least migration has happened across the Alps between Southern France and Italy.

3. Neutral divergence threshold

Differentiation among population pairs calculated from 105,022 1 kb-windows along the genome was very low, with mean F_{ST} ranging from 0.032 to 0.111 (Supporting information S1 Tab. S5). Distribution of pairwise F_{ST} in these windows showed a weak isolation-by-distance pattern between populations (Fig. 3), though insignificant in Mantel's test (ade4 package, R-Core 2015, 999 random permutations, p = 0.21). Comparing the empirical data with the distribution from the simulated drift expectation reveals a distinct mismatch of the data sets, especially for more diverged population-pairs (Fig 3, Supporting information S1 Fig. S4). The *constant* model clearly underestimated the differentiation among all populations, since the distributions peaked around zero. Observed empirical density functions were not comparably approximated by any model, i.e. even with increased complexity accounting for inferred population growth, adjusting for inferred population sizes and migration rates the *growth* and *approximated* model were unable to predict observed neutral divergence among populations.

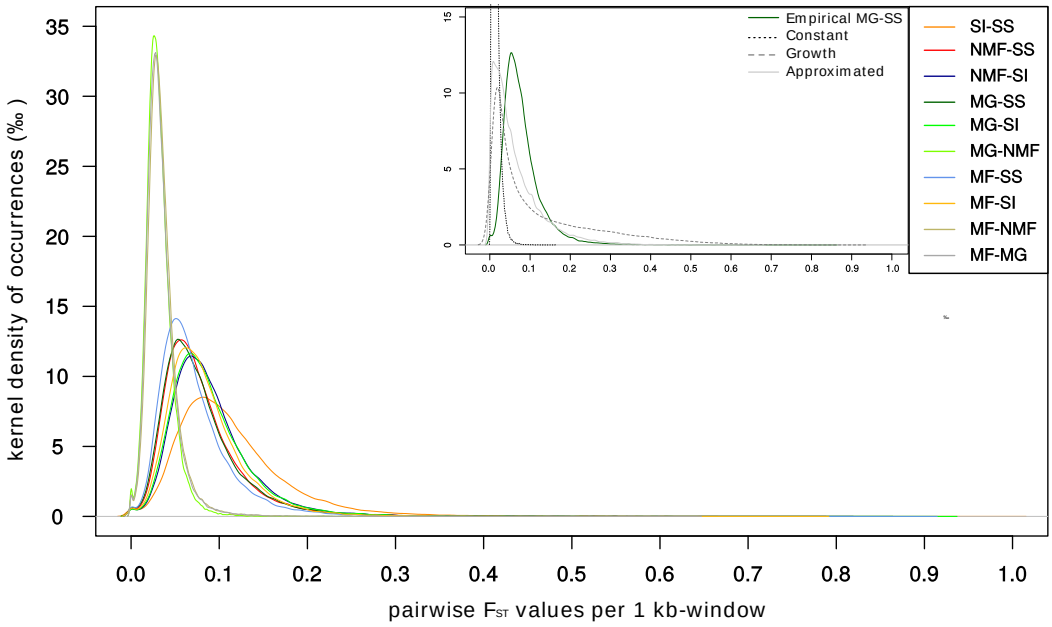

Figure 3: Distribution of pairwise F_{ST} per 1 kb-windows from *C. riparius* Pool-Seq data. Population comparisons are shown with different colours. The integrated graph shows one exemplary population-pair (MG-SS) in comparison to the respective simulated data from three different models.

We therefore decided for the overall more conservative upper 1 % tail of the empirical F_{ST} distribution as neutral divergence threshold for downstream analyses (see discussion below). Statistical F_{ST} thresholds of empirical data and those gained from the *approximated* model were most similar

(Supporting information S1 Tab. S6). However, the statistical threshold from the empirical data was higher and thus more stringent in 7 out of 10 population comparisons. The retained statistical F_{ST} threshold (upper 1 % tail of the distribution) ranged from 0.1 to 0.36 for the respective population-pairs. A total of 4,360 highly diverged 1 kb-windows fell above the F_{ST} threshold from population comparisons (cf. Supporting information S1 Tab. S6 for pairwise numbers), of which 1,161 1 kb-windows were annotated to unique genes.

4. Signatures of selection in highly divergent regions and genomic distribution

Genome-wide averages of Tajima's D (T_D) of 1 kb-windows with low differentiation (lower 99 % tail of the F_{ST} distribution) of all populations levelled around zero (in a range of -1.63 to 1.75, Supporting information S1, Fig. S5), indicating the major influence of neutral processes in shaping the genome. Compared to that neutral background, distribution of T_D was only slightly broader in outlier 1 kb-windows (upper 1 % tail). Purifying selection was found to act on the majority of outlier windows (note that this value cannot be inferred population-wise). Occurrences of selective sweeps and balancing selection differed among populations (Fig. 4). Northernmost and southernmost populations (MG, NMF, SS) showed major impact of ongoing sweeps (significantly different to MF and SI, Supporting information S1, Tab. S7). Balancing selection was significantly increased in the two Southern populations (SI, SS, see Supporting information S1, Tab. S7 for p-values).

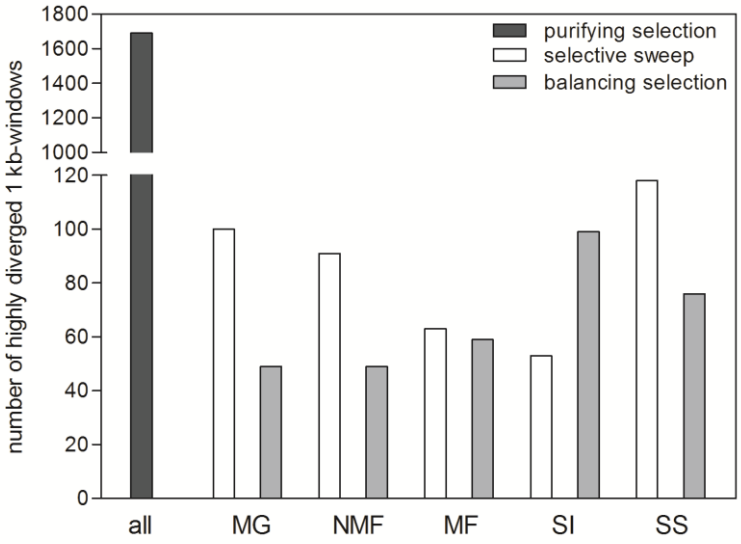

Figure 4: Occurrences of molecular signatures of selection in highly diverged 1 kb-windows of five natural *C. riparius* populations. Refer to Supporting information S1 Table S7 for statistical comparisons.

Joining adjacent 1 kb outlier windows of population-pairs to larger divergence regions resulted in 3,338 1 kb diverged windows above the 5 % F_{ST} cut-off, 1,711 of which could be joined to divergence regions larger than 2 kb. On average, a divergence region was 2478 bp long (± 9764 bp) with a maximum length of 89 kb. Long divergence windows mostly occurred only once with the overall length distribution being strongly left skewed (Supporting information S1, Fig. S6). The mean distance between divergence windows on the same scaffold was more than 80 kb (± 151 kb, Supporting information S1, Fig. S7).

5. Partitioning among clinal and local adaptation

Environmental association analysis with LFMM was calculated on all 149,474 SNPs falling above the 99 % F_{ST} threshold of SNP-based genome-wide population comparisons (not to be confused with the 1 kb-window based population comparisons). Median z-scores were corrected with the estimated inflation factor λ for each of the three environmental variables ($\lambda_{precipitation}$= 0.67, λ_{temp_warm}= 0.71, λ_{temp_cold}= 0.71). The three separate LFMM runs per climate variable resulted in 19,720 SNPs related to the precipitation gradient, 16,956 SNPs related to the gradient of warm temperatures, and 22,959 SNPs related to the gradient of cold temperatures.

Annotation of clinal SNPs resulted in 1,551 unique genes as candidates for clinal adaptation: of those, 49 genes were private to the precipitation gradient, 196 genes private to the warm temperatures gradient, and 47 genes private to the cold temperatures gradient (Supporting information S1, Fig. S8-A). The intersection of these candidates for clinal adaptation with those genes present within the annotated 1 kb-windows from the population comparisons (see above 1,161 genes) resulted in 162 genes (1.2 % of the annotated protein coding genes; Supporting information S1, Tab. S8; Supporting information S3). These 162 clinal candidate genes have statistical support to be significantly diverged between at least two populations and were additionally found to be significantly correlated to one of the climate gradients (Supporting information S1, Fig. S8-B). The intersection furthermore revealed 999 unique genes without clinal character (7.6 % of the annotated protein coding genes, Supporting information S1, Tab. S8; Supporting information S3), as candidates for pure local adaptation.

Based on these different sets of candidate genes, we performed the GO term enrichment analysis to gain insight in biological processes that are likely to be involved in the adaptive evolution to local factors or climate factors (Fig. 5). Among the 999 genes putatively associated with local adaptation, the number of significantly enriched GO terms varied among populations from six in the Rhône-Alpes population (MF) to 19 in the Andalusian population (SS, Supporting information S1, Tab. S8). Associated to the 162 significant candidate genes for clinal adaptation, ten GO terms were found significantly enriched (Supporting information S1 Tab. S8). Especially, significant enrichment of the terms 'apoptotic process' and 'response to heat' provide a valid basis for interpretation. On a deeper level, we found significantly enriched GO terms among candidate genes associated to the three different climate factors (Supporting information S1 Tab. S8). When associating gene hits to their respective KEGG pathways, there was a broad overlap of local and clinal signals (Supporting information S3).

Discussion

1. Thermal adaptation of fitness-relevant traits in *C. riparius*

We experimentally demonstrated fitness-relevant thermal adaptation on the phenotypic level of five natural *C. riparius* populations sampled along a climatic gradient across Europe. According to the temperature conditions of their origin, population growth rate (PGR) of populations from colder sites in the North (annual mean temperature - AMT 9.7 - 9.9°C) were higher at low test-temperatures, compared to populations from warmer sites in the South (AMT 12.1 – 16.5°C), whereas the opposite was true for warm test-temperatures (Fig. 1). This result is in line with previous findings of *C. riparius* populations from different locations among which the variability of PGR could be explained by a mixed effect of genetic drift, genetic diversity, and adaptation to the average temperature during the warmest month (Nemec *et al.* 2013). In *D. melanogaster*, heat and cold resistance differed between temperate and tropical populations (reviewed in Hoffmann & Weeks 2007) in the same clinal direction as found for *C. riparius* populations.

The contribution of traits underlying the PGR as composite fitness measure was different for the two extreme test-temperatures. Low temperatures significantly affected survival during the larval development and reduced viability of the offspring in warm-adapted populations, i.e. significantly less fertile clutches in at least two populations from warmer sites (Supporting information S1, Fig. S3-C). High temperatures did not generally increase mortality in cold-adapted populations or directly affected their fertility, even though variability of these traits increased.

It took more than two decades of research (e.g. Gilchrist *et al.* 1997; Hoffmann *et al.* 2002; Hoffmann & Watson 1993; Parson 1977) to identify decisive phenotypic traits responding to heat and cold selection in *Drosophila*, that is the heat knockdown resistance (time until flies are knocked down by heat in small tubes) and chill coma recovery (recovery time of flies after a cold shock). A direct correlation of fitness traits with population origin and test-temperature thus provides a meaningful model for the investigation of thermal adaptation on all levels (Hereford *et al.* 2004), a correlation that we found in *C. riparius* populations based on the PGR as integrated fitness measure. Since our natural populations have been acclimatised to laboratory conditions for up to three generations, the differential

response to thermal regimes in the experiments was most likely due to heritable differences, thus providing the necessary evidence to search for the genomic basis of this adaptation (Savolainen 2011).

2. Population genetic simulations underestimate neutral divergence in *C. riparius*

Different evolutionary forces, i.e. selection, genetic drift, gene flow, and mutation, simultaneously shape the evolution of populations (Savolainen *et al.* 2013). Signatures of selection can therefore only be identified when patterns of neutral or endogenous evolution are subtracted from the signal of population differentiation, most importantly the impact of demography, migration, and potential endogenous selection barriers (Bierne *et al.* 2011; Flatt 2016). A previous study could show that a special transposable element might act as endogenous genetic barrier among the same European *C. riparius* populations as investigated here, though this pattern was not correlated to classical SNP differentiation between populations (Oppold *et al.* 2017 in press) and can hence be neglected.

A common and proven approach to infer selection is to search for loci with increased population differentiation using F_{ST}-based outlier tests (Narum & Hess 2011). The general idea is that loci in which different alleles are selectively favoured in different populations should exhibit larger allele frequency differences between populations than purely neutrally evolving loci (Beaumont 2005). The challenge remains to identify a divergence threshold above which the influence of neutral processes can be reasonably excluded. This threshold can either be derived in a model-based approach simulating neutral divergence (De Mita *et al.* 2013) or with a statistical threshold derived from the empirical F_{ST} distribution (Beaumont & Balding 2004; Pfenninger *et al.* 2015).

Using the genome-wide inference of N_e history (MSMC analysis, Fig. 2A), estimated migration rates between neighbouring populations (gene flow analysis, Supporting information S2), and the spontaneous mutation rate of *C. riparius* (Oppold & Pfenninger 2016), we parameterised a species-specific population genetic model to simulate the actual drift-expectation in terms of F_{ST} distributions. Despite our substantial effort to obtain realistic empirical parameter estimates and therewith model neutral divergence among the populations, all applied models failed to reproduce the empirical F_{ST} distribution. The simulated data consistently underestimated population differentiation and their 99 % quantile F_{ST} thresholds were unrealistically low (Fig. 3). This could have several, mutually not exclusive reasons: (1) inadequacy of current coalescence/population genetic models for estimation of

gene flow and N_e to account for differential evolutionary speed of populations; (2) pervasive action of selection throughout the entire genome; (3) clinal differentiation could include chromosomal inversion polymorphisms that disproportionately increase population differentiation; (4) cryptic introgression in parts of the species range.

(1) The number of generations per year of a *C. riparius* population strongly depends on the temperature level and course throughout the year (Oppold *et al.* 2016). This leads to substantially different 'evolutionary speeds' among populations of different temperature regions with up to 3-fold different numbers of generations per year. Population genetic consequences of this temperature dependence are, however, not accounted for in current population genetic models used e.g. for coalescence analysis of demography and migration. The coalescence approach uses historical recombination events to infer past population sizes from the distribution of coalescence times (Ellegren & Galtier 2016). The inference is based on a uniform time index for coalescence events, i.e. an equal number of generations. It is currently not possible to correct for this and thus, their coalescence is fundamentally biased. Results of the MSMC analysis for the inference of N_e include this bias as soon as populations were separating from each other and when they are expected to have experienced different temperature regimes (see discussion below). N_e estimates of the recent past and the timing of separation events might thus be incorrect. Similarly, results of the gene flow analysis are based on the distribution of SNPs among populations. Populations from warmer regions can accumulate more polymorphisms while passing more generations (Oppold *et al.* 2016), which in turn might lead to an inflated migration rate estimate towards populations of cooler temperature regions (see discussion below).

(2) Pervasiveness of selection could, in principle, explain the observed discrepancy between simulated and empirical data. In this case, selection of polygenic traits would exert selection on the majority of loci across the genome, thus resulting in a general shift of F_{ST} distributions to higher values. Evidence for such a scenario comes from investigations comparing *Drosophila* species suggesting that most of the genome is under selection (Sella *et al.* 2009). However, our study compared intraspecific *C. riparius* populations with high gene flow and therefore pervasive divergence appears rather unlikely.

(3) There are many cases of inversion polymorphisms with clinal frequency patterns described in *Drosophila* that are correlated to environmental factors or even seasonal climate variations (Kapun *et al.* 2016). Such structural mutations may lead to strong signals of divergence along the inverted sequence between populations. Inversions were described also for many *Chironomus* species, although such polymorphisms were hardly observed in *C. riparius* (then called *C. thummi*, Acton 1956). Furthermore, divergent regions among *C. riparius* are on average rather short (2,478 bp; Supplementary information S1, Fig. S6) and widely distributed (on average 80 kb; Supplementary information S1, Fig. S7), whereas inversions are expected to span large regions along chromosomes (Caceres *et al.* 1997). It is therefore unlikely, though cannot be entirely ruled out, that inversions are involved in the clinal differentiation or even enhance thermal adaptation in *C. riparius* similarly as documented for *Drosophila*.

(4) A scenario of differential introgression from related *Chironomus* species is possible. Whole genome sequencing revealed reticulated evolution across the entire species tree, and hybridization with introgression among related multicellular eukaryotic species seems to be pervasive (Mallet *et al.* 2016; Shapiro *et al.* 2016). Hybridization between *Heliconius* species appears to be a natural phenomenon and Mallet *et al.* (2007) even deduced that introgression may often contribute to adaptive evolution. The genus *Chironomus* is very species-rich and more than 4,000 species are unambiguously aquatic during larval development, often dominating aquatic insect communities (Ferrington 2008), such that larvae of many different species can co-occur at the same location (Pfenninger et al. 2007). The closest relative to *C. riparius* is the morphologically cryptic sister-species *C. piger* that shares habitats (Schmidt *et al.* 2013). Hybridisation of these species is possible under laboratory conditions (Keyl 1963 and own observations), though previous studies found little if any evidence for ongoing hybridisation in the field (Hägele 1999; Pfenninger & Nowak 2008; Pfenninger *et al.* 2007). Experimental analysis of niche segregation between the sister-species showed that *C. riparius* had a higher fitness at higher constant temperatures and larger daily temperature ranges (Nemec *et al.* 2012). It is thus likely that the distribution range of *C. riparius* stretches further South in Europe, overlapping with the *C. piger* range only in more temperate Northern regions. Indeed, *C. piger* was only found in the two Northern-most populations

during sampling for this study. The discrepancy between empirical and simulated F_{ST} distributions was especially large in comparisons with those two Northern populations. A potential differential *C. piger* introgression along the cline of *C. riparius* distribution can thus not be excluded, but requires deeper investigation.

Since it was, for the above potential reasons, not possible to derive a reasonable model-based neutral divergence threshold, we resorted to a statistical threshold as advocated e.g. by Beaumont (2005). These thresholds were in addition more conservative (i.e. higher F_{ST}) for the majority of pairwise comparisons.

3. Demographic population history

The genome-wide inference of population history (MSMC analysis) indicated one ancestral panmictic *C. riparius* population that started diverging approximately 10,000 generations ago until populations reached almost complete separation 1,000 generations ago (Fig. 2B). As long as coalescence analysis indicates a single panmictic population and early population separation, the above discussed influence of evolutionary speed on inference of demographic history should be neglectable. Nevertheless, due to the temperature dependence of generation time it is difficult to convert the scaling of generations to an absolute time scale in years, neither knowing the precise population location nor thermal conditions at that time. Based on previous modelling of the potential number of generations per year at thermal conditions during the last glacial maximum (Oppold *et al.* 2016), we can roughly assume five to eight generations per year for the ancestral panmictic population. This converts the period of population separation to a time horizon from 2000 – 1250 years ago until the last 200-125 years. Associated with the process of population separation, N_e drastically increased. Migration analysis indicated that gene flow radiated from the current Lyon population towards the other populations, even though this result has to be regarded carefully due the above discussed fundamental bias of the estimation. Disregarding absolute migration rates, the general migration pattern suggests that an expansion across Europe might have originated from central France (Supporting information S2).

C. riparius is known for its broad ecological tolerance, yet larvae preferably inhabit rivers with organic pollution (Armitage *et al.* 1997; Groenendijk *et al.* 1998). The increase in population size and potential expansion across Europe might therefore be correlated to the increase in human settlements

(Antrop 2004) and anthropogenic impact (intensification of agriculture, industrialisation, increase in waste water) on the environment in general, and water bodies in particular.

By the time population separation was completed, we can assume that our populations had established their current geographic distribution across Europe, inevitably experiencing different temperature regimes. Demography estimates from the recent past were therefore probably biased and were not applied in downstream analyses. In general, this adds a cautionary note to the analysis of demographic processes in multivoltine ectotherms.

4. Signatures of selection across the species range

Applying the more conservative statistical threshold of the empirical F_{ST} distribution, we focussed on genomic regions that were highly diverged among populations. These regions can be expected to carry distinct signatures of selection and therefore negative Tajima's D values are unlikely to result from neutral demographic processes as expansion, contraction or bottlenecks. Significantly more signatures of ongoing selective sweeps were found in the two Northern populations (MG, NMF) and the southernmost population (SS, Fig. 4; Supporting information S1, Tab. S7). Since we can exclude a significant difference in N_e between populations (Fig. 2A), this pattern suggests that positive selection has been playing a major role in populations at the outer margins of the investigated climatic gradient. Referring back to the hypothesis that populations expanded from central France, i.e. the centre of the thermal cline, might provide an explanation for this spatial pattern of selective sweeps. According to the surfing mutation phenomenon, mutations occurring at the edge of the range expansion are lost at a reduced rate and can more easily be driven to fixation (Klopfstein *et al.* 2006). Therefore, the time of population range expansion is an evolutionary important period, where mutations can accumulate and contribute to adaptation processes. However, the existence of spatial and even temporal heterogeneity in the intensity and direction of selection is known from other species (Bergland *et al.* 2014; Charbonnel & Pemberton 2005). This could furthermore explain the observed spatial difference in the proportion of balancing selection.

5. Functional basis of local and clinal adaptation in *C. riparius*

By combining a F_{ST} outlier approach to characterise population differentiation with an environmental association analysis, it was possible to disentangle the signatures of local and clinal adaptation. While climate factors produce a spatially continuous selection regime, there are additional local selection pressures that act on populations in their specific habitat. *C. riparius* larvae inhabit small ditches and streams with increased carriage of organic matter, mostly in agricultural areas or streams receiving waste effluents from urban areas (Armitage *et al.* 1997; Calle-Martínez & Casas 2006). Consequently, *C. riparius* populations can adapt to their local pollutants, i.e. pesticides (Müller *et al.* 2012), metals (Pedrosa *et al.* 2017; Wai *et al.* 2013), organic pollution (Vogt *et al.* 2007a), and its effects on physicochemical conditions of the water body as decreased oxygen content or hydrogen sulphide levels. Genes overall associated to local adaptation (i.e. found in more than one population but without clinal pattern, Fig. 5: left part, top hierarchy) were significantly enriched with GO terms linked to transport processes, like 'ion transport' and 'intracellular protein transport', especially with association to the endoplasmic reticulum and the Golgi apparatus (Fig. 5, Supporting information S3). Golgi vesicles play important roles in cellular detoxification processes, especially transformation and exocytosis of metals, as shown for a wide range of invertebrate species (Simkiss & Taylor 1989). During cellular detoxification of pesticides several intermediate steps involve phosphorylation or dephosphorylation of proteins (Quistad *et al.* 2000), processes whose GO terms were also significantly enriched on a local scale ('protein phosphorylation' and 'protein dephosphorylation'), though this broad biological process currently cannot be interpreted more mechanistically. Significantly enriched GO terms private to the different populations (Fig. 5) provided insight into habitat-specific adaptive processes. 'Methylation' and 'ATP-dependent chromatin remodelling' were significantly enriched in the Italian population (SI), suggesting an adaptation of the epigenetic system that involves DNA methylation and chromatin modifications. Evidence suggests that insecticide sensitivity in insects might be regulated by epigenetic mechanisms (Oppold *et al.* 2015). Therefore, genetic adaptations interacting with the epigenetic machinery might be a response to insecticide stress on a local scale. In the Hessian and Andalusian population (MG and SS), genes associated to 'Toll signalling pathway' were significantly enriched. In *Drosophila*, Toll receptors are essential for embryonic development

and immunity (Valanne *et al.* 2011). Similarly, candidate genes for local adaptation of the Andalusian population were significantly enriched for 'ecdysone-receptor signalling' that is essential for the coordination of development, molting and metamorphosis (Schwedes & Carney 2012).

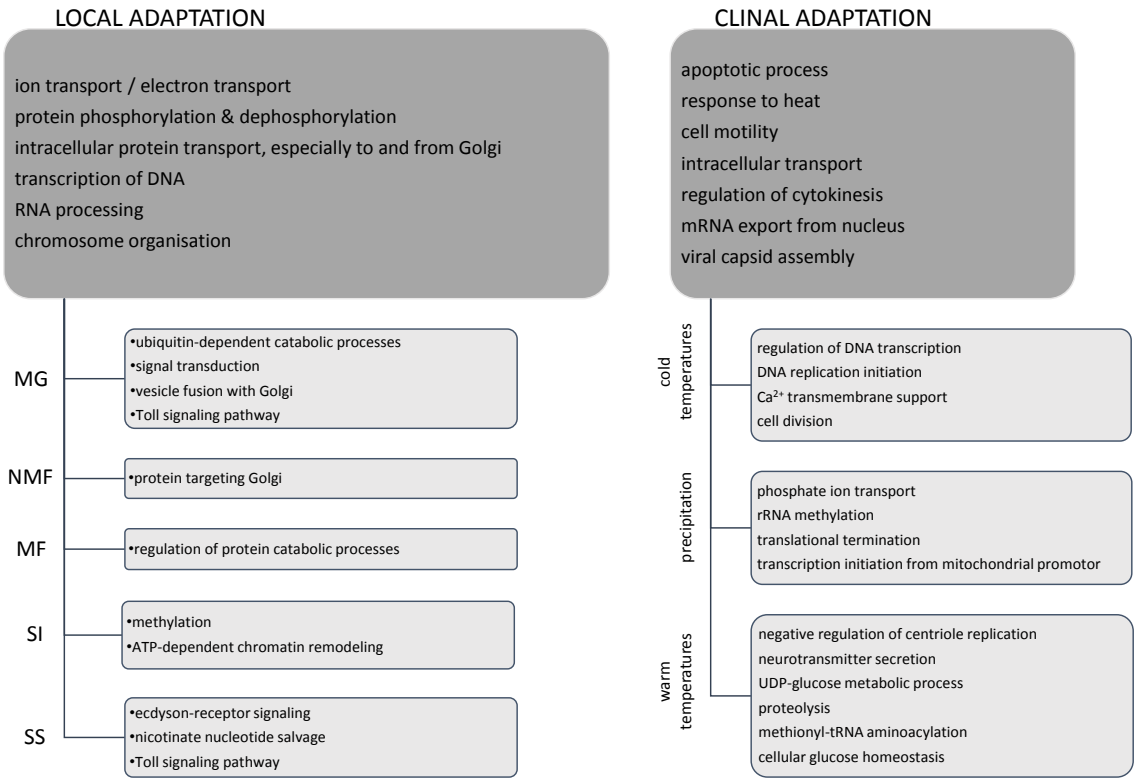

Figure 5: Functionally enriched GO terms associated to disentangled candidate genes for signatures of local adaptation in natural *C. riparius* populations (relevant and private GO terms shown, for complete lists cf. Supplementary Information S3) and for signatures of clinal adaptation along the climatic gradient across Europe. GO terms significantly enriched superior to the respective subgroups at top hierarchy, significantly enriched GO terms specific for subgroups below.

Climatic gradients constitute predictable continuous clines that enable the investigation of clinal adaptation if genotypic variation correlates with the gradual pattern (Adrion *et al.* 2015). The intersection of candidate gene lists from the two different approaches (F_{ST} outliers and candidates from the EAA) resulted in 162 candidate genes that are significantly diverged among populations as well as significantly correlated to the environmental cline. Therefore, 1.2 % of all protein coding genes were probably shaped by climatic selection pressures (Supporting information S1, Tab. S6). The overall response to climatic factors involved the significantly enriched GO term 'apoptotic process' (Fig. 5). Relevant gene hits for this GO annotation include: an apoptosis inhibitor known in *D. melanogaster*, the serine/threonine-protein kinase hippo (Q8T0S6, Harvey *et al.* 2003); the human cell division cycle and apoptosis regulator protein 1 CCAR1 (Q8IX12, Rishi *et al.* 2003); a regulator of proteasomal

degradation and apoptosis known in *Mus musculus*, the E3 ubiquitin-protein ligase HUWE1 (Q7TMY8, Liu *et al.* 2005). Considering the physiological impact of temperature in particular, the necessity to adapt the programmed cell death under stress conditions seems reasonable for ectotherms in general. Moreover and seemingly important for thermal adaptation, the GO term 'response to heat', i.e. any process to change state and activity of molecular processes, was significantly enriched. The herewith associated gene 'transient receptor potential channel pyrexia' may be of special importance, since it is responsive to high temperatures and therefore involved in protection and tolerance from high temperature stress in *D. melanogaster* (Q9W0T5, Lee *et al.* 2005). With the general temperature dependence of biochemical processes, physiological processes on a molecular level are accelerated with increasing temperature (Clarke & Fraser 2004; Gillooly *et al.* 2001). Physiological homeostasis at higher or extreme temperatures thus reasonably requires adaptations on the genetic level.

Adaptation of any process that activates or increases the frequency, rate or extent of the division of the cytoplasm of a cell, and its separation into two daughter cells (GO term 'cell division', e.g. gene hit SPECC1L, a protein involved in cytokinesis and spindle organisation known in *Gallus gallus*, Q2KN97) might buffer cell proliferation at temperature extremes. Similarly, survival of *D. melanogaster* in lines evolved at 14 °C was determined by cytoplasmic factors (Stephanou & Alahiotis 1983) and, accordingly, in *C. riparius* the GO term 'regulation of cytokinesis' was significantly enriched among genes associated to the gradient of cold temperatures.

Warm temperatures, or even heat shock affect protein stability and cells have to cope with stress-induced protein denaturation (Feder & Hofmann 1999). Adaptation of the proteolysis machinery might be a response to the upper temperature extremes along the thermal cline, as indicated by the significantly enriched GO term 'proteolysis' among genes associated to the gradient of warm temperatures (e.g. the *D. melanogaster* protein roadkill that promotes degradation processes by the proteasome, Kent *et al.* 2006). The finding of increased ^{35}S-methionine in the ovaries of female *D. melanogaster* (Stephanou & Alahiotis 1983) and the temperature-sensitivity of the methionyl-t-RNA synthetase (Q9VFL5, Jakubowski & Goldman 1993) might furthermore explain significant enrichment of 'methionyl-t-RNA aminoacylation' in our species among genes associated to warm temperatures.

'Phosphate ion transport' was a significantly enriched GO term among genes associated to the precipitation cline, as e.g. the regulator of ionic currents serine/threonine-protein phosphatase with EF-hands 2 known in *Mus musculus* (O35385). This might be related to osmoregulatory processes in the aquatic larvae due to water level dependent fluctuations of salt concentrations. In insects the water balance is regulated via insect diuretic hormones (Coast *et al.* 2002) and we accordingly found the diuretic hormone receptor (Q16983, *Acheta domesticus*) in the list of precipitation candidates. Competition strength of *C. riparius* larvae against the co-occurring sister species *C. piger* was found to be correlated to precipitation of the warmest quarter/month and in particular negatively correlated to water conductivity, nitrate, and calcium carbonate (Pfenninger & Nowak 2008). This indicates the relevant fitness effect of water composition, as direct result of varying precipitation levels, for *C. riparius* larvae and thus driving adaptation along the precipitation cline.

Association of candidate genes to their respective KEGG pathways showed that on this level of biological organisation locally and clinally adapted processes involved an overlapping combination of pathways (Supporting information S3). Candidate genes for local adaptation as well as clinal adaptation are both involved in metabolism of carbon, nitrogen, methane, and sulphur. Thus, signatures of local and clinal adaptation do not seem to allow a clear separation on the complex level of molecular pathways. Nevertheless, most KEGG pathways could be annotated to candidates for adaptation to warm temperatures (Supporting information S1 Tab. S7), including citrate cycle and calcium signalling pathway, whereas only two pathways ('proteoglycans in cancer' and 'TGF-beta signalling pathway') were annotated to candidate genes of the precipitation gradient.

6. Conclusions

Climate poses a fundamental influence on evolutionary dynamics of multivoltine ectotherms, which becomes apparent in population genetic modelling of their neutral genetic divergence. With our integrative analysis on the phenotypic and genotypic level, we were able to separate the footprints of clinal climate adaptation from habitat-specific local adaptation as well as from neutral evolution among *C. riparius* populations. The comparison of the investigated natural populations revealed the impact of adaptive evolution despite high levels of gene flow and thus on average weak population differentiation. Important biological processes (GO term 'response to heat' or 'apoptotic process')

were identified to be involved in climate adaptation. Deeper investigations on the gene level will be necessary to clarify the decisive genetic factors that underlie those adapted biological processes.

Acknowledgement

We thank Stephan Schiffels and Olivier Francois for help and recommendations on our MSMC2 analysis and LFMM analysis, respectively. We also thank Bob O'Hara for comments and support with the population genetic modelling. Funding was provided by DFG (PF390/8-1). Ann-Marie Oppold acknowledges funding within a scholarship of the FAZIT-Stiftung.

Data accessibility

Raw data from whole genome individual resequencing available at European Nucleotide Archive (ENA project number pending).

Authors' contribution

M.P., T.H., and A.-M.O. conceived the study; A.-M.O. performed common-garden experiments, prepared sequencing of individual resequencing data, phased individual resequencing data and performed MSMC2, and analysed Pool-Seq data; A.-M.O. and M.P. performed the Tajima's D analysis, A.W. and M.P. performed population genetic modelling; A.-M.O. and A.W. performed environmental association analysis; M.P. performed gene flow analysis; B.F. performed functional enrichment analysis; T.S. provided bioinformatic support and custom scripts; S.P. supported Pool-Seq analyses; H.S. supported genomic analyses; A.-M.O., A.W., M.P., B.F., H.S., S.P., and T.H. drafted the manuscript.

References

Acton AB (1956) Chromosomal polymorphism in *Chironomus*. *Proc R Soc Lond B Biol Sci* **145**, 347-350.

Adrion JR, Hahn MW, Cooper BS (2015) Revisiting classic clines in *Drosophila melanogaster* in the age of genomics. *Trends in Genetics* **31**, 434-444.

Alexa A, Rahnenführer J (2016) topGO: Enrichment Analysis for Gene Ontology. In: *Annales de Limnologie - International Journal of Limnology*, p. R package. Bioconductor.

Antrop M (2004) Landscape change and the urbanization process in Europe. *Landscape and Urban Planning* **67**, 9-26.

Armitage P, Cranston PS, Pinder LCV (1997) *The Chironomidae: The biology and ecology of non-biting midges* Chapman & Hall, London.

Beaumont MA (2005) Adaptation and speciation: what can F_{ST} tell us? *Trends in Ecology & Evolution* **20**, 435-440.

Beaumont MA, Balding DJ (2004) Identifying adaptive genetic divergence among populations from genome scans. *Molecular Ecology* **13**, 969-980.

Beerli P (2006) Comparison of Bayesian and maximum-likelihood inference of population genetic parameters. *Bioinformatics* **22**, 341-345.

Beerli P, Felsenstein J (2001) Maximum likelihood estimation of a migration matrix and effective population sizes in n subpopulations by using a coalescent approach. *Proceedings of the National Academy of Sciences of the United States of America* **98**, 4563-4568.

Benjamini Y, Hochberg Y (1995) Controlling the False Discovery Rate - a Practical and Powerful Approach to Multiple Testing. *Journal of the Royal Statistical Society Series B-Methodological* **57**, 289-300.

Bergland AO, Behrman EL, O'Brien KR, Schmidt PS, Petrov DA (2014) Genomic Evidence of Rapid and Stable Adaptive Oscillations over Seasonal Time Scales in *Drosophila*. *Plos Genetics* **10**.

Bergland AO, Tobler R, Gonzalez J, Schmidt P, Petrov D (2016) Secondary contact and local adaptation contribute to genome-wide patterns of clinal variation in *Drosophila melanogaster*. *Molecular Ecology* **25**, 1157-1174.

Bierne N, Welch J, Loire E, Bonhomme F, David P (2011) The coupling hypothesis: why genome scans may fail to map local adaptation genes. *Molecular Ecology* **20**, 2044-2072.

Bolger AM, Lohse M, Usadel B (2014) Trimmomatic: a flexible trimmer for Illumina sequence data. *Bioinformatics* **30**, 2114-2120.

Bukowicki M, Franssen SU, Schlötterer C (2016) High rates of phasing errors in highly polymorphic species with low levels of linkage disequilibrium. *Mol Ecol Resour* **16**, 874-882.

Caceres M, Barbadilla A, Ruiz A (1997) Inversion length and breakpoint distribution in the *Drosophila buzzatii* species complex: Is inversion length a selected trait? *Evolution* **51**, 1149-1155.

Calle-Martínez D, Casas JJ (2006) Chironomid species, stream classification, and water-quality assessment: the case of 2 Iberian Mediterranean mountain regions. *Journal of the North American Benthological Society* **25**, 465-476.

Charbonnel N, Pemberton J (2005) A long-term genetic survey of an ungulate population reveals balancing selection acting on MHC through spatial and temporal fluctuations in selection. *Heredity (Edinb)* **95**, 377-388.

Clarke A (2003) Costs and consequences of evolutionary temperature adaptation. *Trends in Ecology & Evolution* **18**, 573-581.

Clarke A, Fraser KPP (2004) Why does metabolism scale with temperature? *Functional Ecology* **18**, 243-251.

Coast GM, Orchard I, Phillips JE, Schooley DA (2002) Insect diuretic and antidiuretic hormones. *Advances in Insect Physiology, Vol 29* **29**, 279-409.

De Mita S, Thuillet AC, Gay L, *et al.* (2013) Detecting selection along environmental gradients: analysis of eight methods and their effectiveness for outbreeding and selfing populations. *Molecular Ecology* **22**, 1383-1399.

de Villemereuil P, Frichot E, Bazin E, Francois O, Gaggiotti OE (2014) Genome scan methods against more complex models: when and how much should we trust them? *Molecular Ecology* **23**, 2006-2019.

Delaneau O, Howie B, Cox AJ, Zagury JF, Marchini J (2013) Haplotype Estimation Using Sequencing Reads. *American Journal of Human Genetics* **93**, 687-696.

Ellegren H, Galtier N (2016) Determinants of genetic diversity. *Nature Reviews Genetics* **17**, 422-433.

Excoffier L, Foll M (2011) fastsimcoal: a continuous-time coalescent simulator of genomic diversity under arbitrarily complex evolutionary scenarios. *Bioinformatics* **27**, 1332-1334.

Excoffier L, Lischer HEL (2010) Arlequin suite ver 3.5: a new series of programs to perform population genetics analyses under Linux and Windows. *Mol Ecol Resour* **10**, 564-567.

Fabian DK, Kapun M, Nolte V, *et al.* (2012) Genome-wide patterns of latitudinal differentiation among populations of *Drosophila melanogaster* from North America. *Molecular Ecology* **21**, 4748-4769.

Feder ME, Hofmann GE (1999) Heat-shock proteins, molecular chaperones, and the stress response: Evolutionary and ecological physiology. *Annual Review of Physiology* **61**, 243-282.

Ferrington LC (2008) Global diversity of non-biting midges (Chironomidae; Insecta-Diptera) in freshwater. *Hydrobiologia* **595**, 447-455.

Flatt T (2016) Genomics of clinal variation in *Drosophila*: disentangling the interactions of selection and demography. *Molecular Ecology* **25**, 1023-1026.

Fraser DJ, Weir LK, Bernatchez L, Hansen MM, Taylor EB (2011) Extent and scale of local adaptation in salmonid fishes: review and meta-analysis. *Heredity (Edinb)* **106**, 404-420.

Frichot E, Francois O (2015) LEA: An R package for landscape and ecological association studies. *Methods in Ecology and Evolution* **6**, 925-929.

Frichot E, Schoville SD, Bouchard G, Francois O (2013) Testing for Associations between Loci and Environmental Gradients Using Latent Factor Mixed Models. *Mol Biol Evol* **30**, 1687-1699.

Futschik A, Schlötterer C (2010) The Next Generation of Molecular Markers From Massively Parallel Sequencing of Pooled DNA Samples. *Genetics* **186**, 207-218.

Gilchrist GW, Huey RB, Partridge L (1997) Thermal sensitivity of *Drosophila melanogaster:* Evolutionary responses of adults and eggs to laboratory natural selection at different temperatures. *Physiological Zoology* **70**, 403-414.

Gillooly JF, Brown JH, West GB, Savage VM, Charnov EL (2001) Effects of size and temperature on metabolic rate. *Science* **293**, 2248-2251.

Groenendijk D, Postma JF, Kraak MHS, Admiraal W (1998) Seasonal dynamics and larval drift of *Chironomus riparius* (Diptera) in a metal contaminated lowland river. *Aquatic Ecology* **32**, 341-351.

Günther T, Coop G (2013) Robust Identification of Local Adaptation from Allele Frequencies. *Genetics* **195**, 205-+.

Hägele K (1999) Hybrid syndrome-induced postzygotic reproductive isolation: A second reproduction barrier in *Chironomus thummi* (Diptera, Chironomidae). *Journal of Zoological Systematics and Evolutionary Research* **37**, 161-164.

Hammer Ø, T. HDA, D. RP (2001) PAST: Paleontological Statistics Software Package For Education And Data Analysis. *Palaeontologia Electronica* **4**.

Harvey KF, Pfleger CM, Hariharan IK (2003) The *Drosophila* Mst ortholog, hippo, restricts growth and cell proliferation and promotes apoptosis. *Cell* **114**, 457-467.

Hereford J, Hansen TF, Houle D (2004) Comparing strengths of directional selection: How strong is strong? *Evolution* **58**, 2133-2143.

Hijmans RJ, Cameron SE, Parra JL, Jones PG, Jarvis A (2005) Very high resolution interpolated climate surfaces for global land areas. *International Journal of Climatology* **25**, 1965-1978.

Hoffmann AA, Anderson A, Hallas R (2002) Opposing clines for high and low temperature resistance in *Drosophila melanogaster*. *Ecology Letters* **5**, 614-618.

Hoffmann AA, Watson M (1993) Geographical Variation in the Acclimation Responses of *Drosophila* to Temperature Extremes. *American Naturalist* **142**, S93-S113.

Hoffmann AA, Weeks AR (2007) Climatic selection on genes and traits after a 100 year-old invasion: a critical look at the temperate-tropical clines in *Drosophila melanogaster* from eastern Australia. *Genetica* **129**, 133-147.

Jakubowski H, Goldman E (1993) Synthesis of Homocysteine Thiolactone by Methionyl-Transfer Rna-Synthetase in Cultured-Mammalian-Cells. *Febs Letters* **317**, 237-240.

Jones P, Binns D, Chang HY, *et al.* (2014) InterProScan 5: genome-scale protein function classification. *Bioinformatics* **30**, 1236-1240.

Kapun M, Fabian DK, Goudet J, Flatt T (2016) Genomic Evidence for Adaptive Inversion Clines in *Drosophila melanogaster*. *Mol Biol Evol* **33**, 1317-1336.

Kent D, Bush EW, Hooper JE (2006) Roadkill attenuates Hedgehog responses through degradation of Cubitus interruptus. *Development* **133**, 2001-2010.

Keyl HG (1963) Crossing over bei Bastarden von *Chironomus thummi* und *Chironomus thummi piger*. *Chromosoma* **13**, 588-599.

Klopfstein S, Currat M, Excoffier L (2006) The fate of mutations surfing on the wave of a range expansion. *Mol Biol Evol* **23**, 482-490.

Kofler R, Orozco-terWengel P, De Maio N, *et al.* (2011a) PoPoolation: A Toolbox for Population Genetic Analysis of Next Generation Sequencing Data from Pooled Individuals. *Plos One* **6**.

Kofler R, Pandey RV, Schlötterer C (2011b) PoPoolation2: identifying differentiation between populations using sequencing of pooled DNA samples (Pool-Seq). *Bioinformatics* **27**, 3435-3436.

Lee Y, Lee Y, Lee J, *et al.* (2005) Pyrexia is a new thermal transient receptor potential channel endowing tolerance to high temperatures in *Drosophila melanogaster*. *Nature Genetics* **37**, 305-310.

Li H, Durbin R (2009) Fast and accurate short read alignment with Burrows-Wheeler transform. *Bioinformatics* **25**, 1754-1760.

Li H, Handsaker B, Wysoker A, *et al.* (2009) The Sequence Alignment/Map format and SAMtools. *Bioinformatics* **25**, 2078-2079.

Liu ZQ, Oughtred R, Wing SS (2005) Characterization of E3(Histone), a novel testis ubiquitin protein ligase which ubiquitinates histones. *Molecular and Cellular Biology* **25**, 2819-2831.

Loya-Rebollar E, Saenz-Romero C, Lindig-Cisneros RA, *et al.* (2013) Clinal variation in *Pinus hartwegii* populations and its application for adaptation to climate change. *Silvae Genetica* **62**, 86-95.

Mackay TFC, Richards S, Stone EA, *et al.* (2012) The *Drosophila melanogaster* Genetic Reference Panel. *Nature* **482**, 173-178.

Mallet J, Beltran M, Neukirchen W, Linares M (2007) Natural hybridization in heliconiine butterflies: the species boundary as a continuum. *Bmc Evolutionary Biology* **7**.

Mallet J, Besansky N, Hahn MW (2016) How reticulated are species? *Bioessays* **38**, 140-149.

McKenna A, Hanna M, Banks E, *et al.* (2010) The Genome Analysis Toolkit: A MapReduce framework for analyzing next-generation DNA sequencing data. *Genome Research* **20**, 1297-1303.

Müller R, Seeland A, Jagodzinski LS, *et al.* (2012) Simulated climate change conditions unveil the toxic potential of the fungicide pyrimethanil on the midge *Chironomus riparius*: a multigeneration experiment. *Ecology and Evolution* **2**, 196-210.

Narum SR, Hess JE (2011) Comparison of F_{ST} outlier tests for SNP loci under selection. *Mol Ecol Resour* **11 Suppl 1**, 184-194.

Nemec S, Hess M, Nowak C, Pfenninger M (2012) Experimental evidence for niche segregation in a sister species pair of non-biting midges. *Hydrobiologia* **691**, 203-212.

Nemec S, Patel S, Nowak C, Pfenninger M (2013) Evolutionary determinants of population differences in population growth rate x habitat temperature interactions in *Chironomus riparius*. *Oecologia* **172**, 585-594.

Oppold A, Kress A, Bussche JV, *et al.* (2015) Epigenetic alterations and decreasing insecticide sensitivity of the Asian tiger mosquito *Aedes albopictus*. *Ecotoxicology and Environmental Safety* **122**, 45-53.

Oppold AM, Pedrosa JA, Balint M, *et al.* (2016) Support for the evolutionary speed hypothesis from intraspecific population genetic data in the non-biting midge *Chironomus riparius*. *Proc Biol Sci* **283**.

Oppold AM, Pfenninger M (2016) Direct estimation of the spontaneous mutation rate by short-term mutation accumulation lines in *Chironomus riparius*. bioRxiv.

Oppold AM, Schmidt H, Rose M, *et al.* (2017 in press) *Chironomus riparius* (Diptera) genome sequencing reveals the impact of minisatellite transposable elements on population divergence. *Molecular Ecology*.

Parson PA (1977) Resistance to cold temperature stress in populations of *Drosophila melanogaster* and *D. simulans*. *Australian Journal of Zoology* **25**, 693-698.

Pedrosa JAM, Cocchiararo B, Bordalo MD, *et al.* (2017) The role of genetic diversity and past-history selection pressures in the susceptibility of *Chironomus riparius* populations to environmental stress. *Science of the Total Environment* **576**, 807-816.

Pfenninger M, Nowak C (2008) Reproductive Isolation and Ecological Niche Partition among Larvae of the Morphologically Cryptic Sister Species *Chironomus riparius* and *C. piger*. *Plos One* **3**.

Pfenninger M, Nowak C, Kley C, Steinke D, Streit B (2007) Utility of DNA taxonomy and barcoding for the inference of larval community structure in morphologically cryptic *Chironomus* (Diptera) species. *Molecular Ecology* **16**, 1957-1968.

Pfenninger M, Patel S, Arias-Rodriguez L, *et al.* (2015) Unique evolutionary trajectories in repeated adaptation to hydrogen sulphide-toxic habitats of a neotropical fish (*Poecilia mexicana*). *Molecular Ecology* **24**, 5446-5459.

Pinder LCV (1986) *Biology of freshwater Chironomidae*.

Quistad GB, Zhang NJ, Sparks SE, Casida JE (2000) Phosphoacetylcholinesterase: Toxicity of phosphorus oxychloride to mammals and insects that can be attributed to selective phosphorylation of acetylcholinesterase by phosphorodichloridic acid. *Chemical Research in Toxicology* **13**, 652-657.

R-Core (2015) R: A language and environment for statistical computing. R Foundation for Statistical Computing, Vienna, Austria.

Rishi AK, Zhang LY, Boyanapalli M, *et al.* (2003) Identification and characterization of a cell cycle and apoptosis regulatory protein-1 as a novel mediator of apoptosis signaling by retinoid CD437. *Journal of Biological Chemistry* **278**, 33422-33435.

Savolainen O (2011) The Genomic Basis of Local Climatic Adaptation. *Science* **334**, 49-50.

Savolainen O, Lascoux M, Merila J (2013) Ecological genomics of local adaptation. *Nature Reviews Genetics* **14**, 807-820.

Schiffels S, Durbin R (2014) Inferring human population size and separation history from multiple genome sequences. *Nature Genetics* **46**, 919-925.

Schmidt H, Greshake B, Feldmeyer B, Hankeln T, Pfenninger M (2013) Genomic basis of ecological niche divergence among cryptic sister species of non-biting midges. *Bmc Genomics* **14**.

Schmidt PS, Zhu CT, Das J, *et al.* (2008) An amino acid polymorphism in the couch potato gene forms the basis for climatic adaptation in *Drosophila melanogaster*. *Proceedings of the National Academy of Sciences of the United States of America* **105**, 16207-16211.

Schwedes CC, Carney GE (2012) Ecdysone signaling in adult *Drosophila melanogaster*. *Journal of Insect Physiology* **58**, 293-302.

Sella G, Petrov DA, Przeworski M, Andolfatto P (2009) Pervasive Natural Selection in the *Drosophila* Genome? *Plos Genetics* **5**.

Sezgin E, Duvernell DD, Matzkin LM, *et al.* (2004) Single-locus latitudinal clines and their relationship to temperate adaptation in metabolic genes and derived alleles in *Drosophila melanogaster*. *Genetics* **168**, 923-931.

Shapiro BJ, Leducq JB, Mallet J (2016) What Is Speciation? *Plos Genetics* **12**.

Silva G, Lima FP, Martel P, Castilho R (2014) Thermal adaptation and clinal mitochondrial DNA variation of European anchovy. *Proceedings of the Royal Society B-Biological Sciences* **281**.

Simkiss K, Taylor MG (1989) Convergence of Cellular-Systems of Metal Detoxification. *Marine Environmental Research* **28**, 211-214.

Stephanou G, Alahiotis SN (1983) Non-Mendelian Inheritance of "Heat-Sensitivity" in *Drosophila melanogaster*. *Genetics* **103**, 93-107.

Valanne S, Wang JH, Ramet M (2011) The *Drosophila* Toll Signaling Pathway. *Journal of Immunology* **186**, 649-656.

Vogt C, Nowak C, Diogo JB, *et al.* (2007a) Multi-generation studies with *Chironomus riparius* - Effects of low tributyltin concentrations on life history parameters and genetic diversity. *Chemosphere* **67**, 2192-2200.

Vogt C, Pupp A, Nowak C, *et al.* (2007b) Interaction between genetic diversity and temperature stress on life-cycle parameters and genetic variability in midge *Chironomus riparius* populations. *Climate Research* **33**, 207-214.

Wai I, Chong K, Ho WS (2013) Influence of heavy metals on glyceraldehyde-3-phosphate dehydrogenase interactions in Chironomus riparius larvae. *Environmental Toxicology and Chemistry* **32**, 1882-1887.

Yampolsky LY, Zeng EL, Lopez J, *et al.* (2014) Functional genomics of acclimation and adaptation in response to thermal stress in *Daphnia*. *Bmc Genomics* **15**.